ANTIMICROBIAL AGENTS AND CHEMOTHERAPY, Mar. 2007, p. 868–876 Vol. 51, No. 3
0066-4804/07/$08.00+0 doi:10.1128/AAC.01159-06

Antiparasitic Drug Nitazoxanide Inhibits the Pyruvate Oxidoreductases of *Helicobacter pylori*, Selected Anaerobic Bacteria and Parasites, and *Campylobacter jejuni*[▽]

Paul S. Hoffman,[1,2,4,5]* Gary Sisson,[4] Matthew A. Croxen,[1,2,4] Kevin Welch,[3] W. Dean Harman,[3] Nunilo Cremades,[6,7] and Michael G. Morash[4]

Department of Medicine, Division of Infectious Diseases and International Health,[1] Department of Microbiology,[2] and Department of Chemistry,[3] University of Virginia, Charlottesville, Virginia 22908; Department of Microbiology and Immunology[4] and Department of Medicine, Division of Infectious Diseases,[5] Faculty of Medicine, Dalhousie University, Halifax, Nova Scotia, Canada B3H 4H7; and Departamento de Bioquímica y Biología Molecular y Celular, Facultad de Ciencias, Universidad de Zaragoza,[6] and Biocomputing and Physics of Complex Systems Institute,[7] Zaragoza, Spain

Received 15 September 2006/Returned for modification 7 November 2006/Accepted 1 December 2006

Nitazoxanide (NTZ) exhibits broad-spectrum activity against anaerobic bacteria and parasites and the ulcer-causing pathogen *Helicobacter pylori*. Here we show that NTZ is a noncompetitive inhibitor (K_i, 2 to 10 μM) of the pyruvate:ferredoxin/flavodoxin oxidoreductases (PFORs) of *Trichomonas vaginalis*, *Entamoeba histolytica*, *Giardia intestinalis*, *Clostridium difficile*, *Clostridium perfringens*, *H. pylori*, and *Campylobacter jejuni* and is weakly active against the pyruvate dehydrogenase of *Escherichia coli*. To further mechanistic studies, the PFOR operon of *H. pylori* was cloned and overexpressed in *E. coli*, and the multisubunit complex was purified by ion-exchange chromatography. Pyruvate-dependent PFOR activity with NTZ, as measured by a decrease in absorbance at 418 nm (spectral shift from 418 to 351 nm), unlike the reduction of viologen dyes, did not result in the accumulation of products (acetyl coenzyme A and CO_2) and pyruvate was not consumed in the reaction. NTZ did not displace the thiamine pyrophosphate (TPP) cofactor of PFOR, and the 351-nm absorbing form of NTZ was inactive. Optical scans and ^{1}H nuclear magnetic resonance analyses determined that the spectral shift (A_{418} to A_{351}) of NTZ was due to protonation of the anion (NTZ^-) of the 2-amino group of the thiazole ring which could be generated with the pure compound under acidic solutions ($pK_a = 6.18$). We propose that NTZ^- intercepts PFOR at an early step in the formation of the lactyl-TPP transition intermediate, resulting in the reversal of pyruvate binding prior to decarboxylation and in coordination with proton transfer to NTZ. Thus, NTZ might be the first example of an antimicrobial that targets the "activated cofactor" of an enzymatic reaction rather than its substrate or catalytic sites, a novel mechanism that may escape mutation-based drug resistance.

Nitazoxanide [2-acetyloxy-*N*-(5-nitro-2-thiazolyl) benzamide] (NTZ) is a broad-spectrum drug that is efficacious for the treatment of infections caused by amitochondriate luminal parasites and helminths (8, 15, 21, 26) and that shows promise as an alternative therapy for treating infections caused by *Clostridium difficile* (20). More generally, NTZ appears to be an effective treatment for persistent diarrhea (35) and even infections caused by rotavirus (26). NTZ shares some structural similarities with thiamine pyrophosphate (TPP) (Fig. 1) and exhibits a spectrum of activity similar to those of metronidazole (MTZ) and nitrofuran drugs (22), but several lines of evidence suggest that this drug is mechanistically different from the redox-active prodrugs (8, 18, 28). For example, NTZ does not increase the mutation frequency or produce DNA damage in *Helicobacter pylori* (28), and there is no cross-resistance with MTZ, as MTZ-resistant strains of *Trichomonas vaginalis* and *H. pylori* remain susceptible to NTZ (1, 18, 28, 34). Unlike MTZ, resistance to NTZ has not been observed clinically or generated by in vitro methods commonly used to isolate MTZ^r mutants of *H. pylori* (18). Despite the ever widening spectrum of activity reported for NTZ and its therapeutic potential, little is known regarding the mechanism(s) of action.

In support of a novel mode of action, our previous studies showed NTZ to be an inhibitor of pyruvate:ferredoxin oxidoreductase (PFOR) of *H. pylori* (28). PFOR catalyzes the oxidative decarboxylation of pyruvate to acetyl coenzyme A (acetyl-CoA) and CO_2, with reducing equivalents transferred to either ferredoxin or flavodoxin (Fig. 2). These enzymes are also found in the amitochondriate eukaryotic human parasites (*Trichomonas vaginalis*, *Entamoeba histolytica*, and *Giardia intestinalis*), *Cryptosporidium parvum*, most anaerobic bacteria (*Clostridium* spp.), archaea, and microaerophiles of the epsilon proteobacterial group. Several MIC-based studies have shown NTZ to be very potent against large numbers of species of anaerobic bacteria, all of which utilize PFOR for the catabolism of pyruvate (5, 22). Importantly, PFORs, which are highly conserved through evolution and in function (13), differ from the NADH-producing pyruvate dehydrogenase (PDH) com-

* Corresponding author. Mailing address: Division of Infectious Diseases and International Health, Room 2146, MR-4 Bldg., 409 Lane Road, University of Virginia Health Systems, Charlottesville, VA 22908-1340. Phone: (434) 924-2893. Fax: (434) 924-0075. E-mail: psh2n@virginia.edu.

▽ Published ahead of print on 11 December 2006.

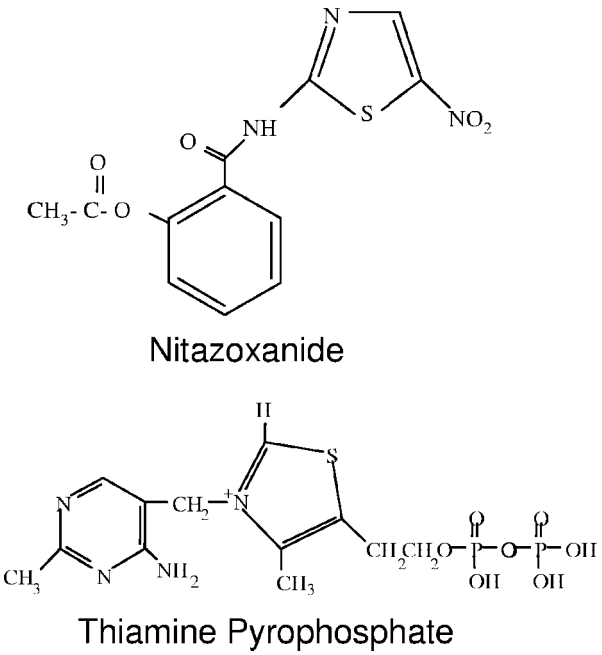

FIG. 1. Structures of nitazoxanide and thiamine pyrophosphate. Solutions of NTZ in DMSO exist in a 10-to-1 ratio of HNTZ to NTZ^-. The form depicted shows the amino group on the thiazole ring as protonated. Figure 9A shows the possible configurations of the protonated forms of HNTZ and various resonance structures of the NTZ^- anion.

plex that is exclusive to mammals and most eubacteria by their requirement for ferredoxin or flavodoxin as electron acceptors (4, 11, 16), by tight binding of thiamine pyrophosphate (TPP) to the enzyme, and by the reversible nature of the enzyme in CO_2 fixation (6).

Here we show that NTZ is a noncompetitive inhibitor of the PFORs of luminal parasites, species of *Clostridium* including *C. difficile*, and the microaerophiles *Campylobacter jejuni* and *H. pylori*. Mechanistic studies with the PFOR of *H. pylori* indicate that NTZ inhibits an early step of the PFOR reaction, since the drug blocks the formation of CO_2 and acetyl-CoA, and the transfer of reducing equivalents to redox-active dyes. ^1H nuclear magnetic resonance (NMR) studies identified two apparent forms of NTZ: a biologically active anion (pK_a = 6.18) and a biologically inactive protonated form of NTZ at lower pH (HNTZ). While NTZ was less efficient in inhibiting the pyruvate dehydrogenase activity of *Escherichia coli* in direct enzyme assays, bacterial growth was substantially inhibited in a glucose minimal medium, suggesting that the microbial spectrum of NTZ for non-PFOR-containing organisms might be influenced by nutrition. NTZ may be the first example of an antimicrobial agent that targets the "activated cofactor" of an enzymatic reaction rather than its substrate or catalytic sites, a potentially novel mechanism that may escape mutation-based drug resistance.

MATERIALS AND METHODS

Bacterial and parasite strains, growth media, and preparation of extracts. The isolates of *E. histolytica* and *T. vaginalis* were obtained from the London School of Hygiene and Tropical Medicine, *G. intestinalis* was obtained from McGill University, and *C. difficile* and *C. perfringens* were obtained from the Department of Microbiology, Dalhousie University. *H. pylori* strain KE26695 and *C. jejuni* H840 have been described previously (9, 11, 28, 32).

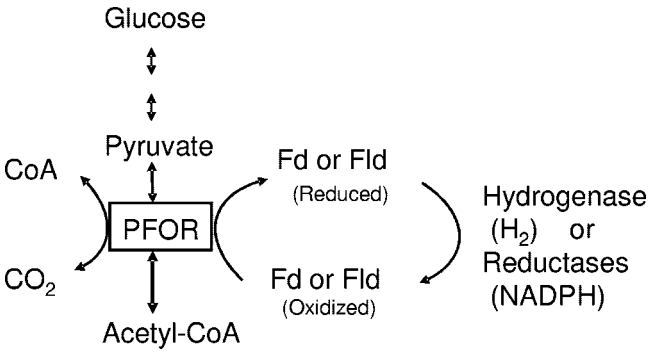

FIG. 2. PFOR reaction. PFOR catalyzes the oxidative decarboxylation of pyruvate, producing acetyl-CoA and CO_2, with ferredoxin (Fd) or flavodoxin (Fld) serving as the electron acceptor. Reduced carriers are oxidized by hydrogenase or NADP oxidases that produce H_2 and NADPH, respectively. The reversible nature of PFOR is indicated by arrows depicting both directions for the enzyme reaction.

Parasites were grown in Diamond's TYI-33 medium, as described previously (1). *Clostridium* species were grown in PYG medium under anaerobic conditions (17), and *H. pylori* was grown in a brucella-based medium (brucella agar) supplemented with 7.5% fetal calf serum and incubated under microaerobic conditions, as described previously (9, 29). *C. jejuni* strain H840 was grown microaerobically on brucella agar (11). MIC determinations for NTZ were done by microdilution in 96-well microtiter plates in brain heart infusion medium supplemented with 2% serum, and the MICs were read at 27 h. *E. coli* strains AV1157 (wild type) and JVQ2 (*nfsA nfsB*) were obtained from I. B. Lambert (33) and were used as host strains for the expression of PFOR from pBluescript (pBSK), as described previously (28).

Parasites were collected from broth cultures by centrifugation at 6,000 × *g* and 4°C for 15 min; and ca. 2 g of paste, suspended in 5 ml of buffer (31), was disrupted by sonication or with a glass homogenizer. Cell debris was removed by low-speed centrifugation (6,000 × *g* for 15 min), and the supernatants were clarified further by centrifugation at 14,000 × *g* for 20 min. Extracts from *T. vaginalis* were prepared as described previously (31). The protein concentration was estimated by the Bradford method (Bio-Rad).

Bacteria were similarly collected by centrifugation and were disrupted by sonication as described previously (28). Bacterial extracts were centrifuged at low speed to remove the cell debris and unbroken cells, and then the supernatants were subjected to ultracentrifugation (100,000 × *g* for 1 h) to obtain a high-speed supernatant that contained PFOR activity.

Cloning, expression, and partial purification of *H. pylori porDCAB*. The *porDCAB* operon was cloned into pBSK and transformed into *E. coli* strain JVQ2 as described previously (28). *E. coli* isolates expressing PFOR were pelleted by centrifugation (6,000 × *g*) for 5 min at 4°C; washed once in phosphate-buffered saline; suspended in buffer A, which contained 50 mM Tris-HCl (pH 7.4), 1 mM $MgCl_2$, 1 mM dithiothreitol, and 10% glycerol; and passaged two to three times through a French pressure cell under nitrogen gas. The crude extract was centrifuged at 10,000 × *g* for 30 min at 4°C to remove unbroken cells and debris and then at 100,000 × *g* for 1 h at 4°C to obtain a high-speed supernatant containing PFOR. The protein concentration was adjusted to 25 mg/ml in buffer A, and the extract was applied to a diethyl-aminoethyl cellulose (DE-52) column equilibrated with degassed buffer A under nitrogen. The PFOR protein was eluted from the column with a sodium chloride gradient prepared in buffer A (0 to 1 M NaCl) that had been degassed and kept under a constant stream of nitrogen. Fractions were collected in stoppered serum bottles under nitrogen, as monitored with a UV monitor (Isco). Samples from each fraction were tested for PFOR activity by a rapid assay (14, 28). PFOR-containing fractions were pooled and subjected to ultrafiltration dialysis (Amicon P30) in buffer A, aliquoted, and either used immediately or stored at −80°C in 10% glycerol. Displacement of the TPP cofactor of PFOR by NTZ was done with 3 mg/ml protein dialyzed against 10 mM NTZ and 10 mM sodium pyruvate in buffer A with 20% dimethyl sulfoxide (DMSO). The suspension was dialyzed three times with an Amicon

10,000-molecular-weight-cutoff spin column. A control PFOR sample was similarly treated with 20% DMSO in buffer A with 10 mM sodium pyruvate.

E. coli strain CC104 harboring either pBSK or pGS950 (a vector expressing the *rdxA* gene of *H. pylori*) were grown in 2% glucose minimal (MinA) liquid medium containing MTZ or NTZ (0, 5, 10, 15 μg/ml), as described previously (28, 29). The turbidities of the cultures (triplicate) at 660 nm were read at 16 h and were normalized to the percentage of the turbidity of the control (no drug).

Enzyme assays. PFOR enzyme assays were carried out at 25°C in 1-ml cuvettes in a modified Cary-14 spectrophotometer equipped with an OLIS data acquisition system (On Line Instrument Co., Bogart, Georgia) (12). PFOR (EC 1.2.7.1) was assayed under anaerobic conditions with 100 mM potassium phosphate (pH 7.4), 10 mM sodium pyruvate, 5 mM benzyl viologen (BV; $\varepsilon = 9.2\ mM^{-1}\ cm^{-1}$ at 546 nm), 0.18 mM CoA, 1 mM $MgCl_2$, and 5 μM TPP. The reaction was started by addition of enzyme, and the reduction of redox-active BV dye was monitored at 546 nm. PFOR was also assayed under anaerobic conditions with NTZ (28) by monitoring the decrease in the absorbance at 418 nm ($\varepsilon = 18.64\ mM^{-1}\ cm^{-1}$). NTZ was prepared as a 20-mg/ml stock solution in DMSO (65 mM). PDH was assayed in extracts from *E. coli* JVQ2 by monitoring the reduction of NAD at 340 nm. The 1-ml reaction mixture contained 150 mM potassium phosphate buffer (pH 8.0), 3 mM sodium pyruvate, 3 mM $MgCl_2$, 0.18 mM CoA, 5 μM TPP, 0.3 mM NAD, and 9 mM L-cysteine. Enzymatic activities are reported as nanomoles or micromoles per minute per milligram of protein. All assays were performed in triplicate, and the mean and the standard deviation were computed. Variations in enzyme activity from batch to batch were also examined in triplicate in bacterial extracts prepared on different days. The protein concentration was estimated by the Bradford method (Bio-Rad).

Kinetic and inhibitor analyses. The initial velocities for PFOR (*H. pylori*) were measured at each concentration of pyruvate (0, 0.05, 0.1, 0.2, 0.4, 1, 5, 10, 20 mM) in the standard assay with either BV or NTZ as the electron acceptor. The NTZ concentration was then varied over a range of concentrations, with the other components present in excess, to obtain kinetic constants. Concentration-dependent inhibition of PFOR activity by NTZ was determined with excess BV (5 mM), initial velocities were determined at each concentration of NTZ (0 to 264 μM), and the decrease in the initial velocity of BV reduction at each concentration of NTZ was measured spectrophotometrically at 546 nm and plotted as $1/V$ versus I (where V is velocity and I is the NTZ concentration [in μM]) for selected organisms or partly purified PFOR.

Determination of acetyl-CoA production. The level of accumulation of acetyl-CoA in the PFOR reaction was determined at various times by removing aliquots of the standard PFOR reaction mixture, which, following treatment with perchloric acid, centrifugation, and neutralization, was added to an enzyme-coupled reaction mixture (19). Briefly, at each time point, 200 μl of neutralized sample was assayed for acetyl-CoA in a total volume of 1.0 ml that contained 200 mM Tris-HCl (pH 8.0), 5 mM malate, 1.5 mM NAD (pH 8.0), 900 mU of malate dehydrogenase (from pig heart; Sigma), and 75 mU of citrate synthase (from pig heart; Sigma). The amount of acetyl-CoA produced was proportional to the initial velocity of NADH formation measured at 340 nm (19). The concentration of acetyl-CoA was determined from a standard curve prepared by the same protocol.

Capture of $^{14}CO_2$. The PFOR enzyme activity was standardized for a stoppered 10-ml Vacutainer tube under anaerobic conditions. The reaction was started by addition of 5 μCi [^{14}C]pyruvate (uniformly labeled). A CO_2 trap (200 μl of a 100 mM NaOH solution) contained in a borosilicate glass transport vial was inserted in the Vacutainer tube. The following electron acceptors were used at the indicated final concentrations: 5 mM BV, 0.02 mM NTZ, 0.02 mM tizoxanide (TIZ; tizoxanide is the deacylated form of NTZ), and 0.02 mM DMSO as a control. Inhibition experiments were set up to determine if NTZ competed with BV and altered CO_2 evolution. An enzyme control was included in which no enzyme was added. Prior to addition of radiolabel, each tube was sparged with a stream of H_2 gas through the rubber stopper to remove the oxygen. Fifty microliters of the NaOH trap contents was added to 5 ml scintillation fluid and counted by liquid scintillation. Blank as well as enzyme control counts were subtracted from the total count, and means and standard deviations were determined.

Pyruvate consumption: LDH assay. To measure the remaining pyruvate in the PFOR reaction, a coupled assay with lactate dehydrogenase (LDH) was used. For these experiments, the starting concentration of pyruvate was decreased to 0.5 mM, with the concentrations of the other reagents remaining the same as those indicated above. Parallel reactions were set up; harvested entirely at 0, 1, 2, 3, 4, and 8 min with NTZ as the electron acceptor and at 0, 0.33, 0.67, 1, 2, and 4 min with BV; and processed as follows. To each sample, ice-cold perchloric acid was added to a final concentration of 500 mM, and the mixture was incubated on ice for 40 min. Samples were then centrifuged for 5 min at 2,800 × *g* and 4°C. The supernatants were neutralized by addition of a one-third volume of saturated $KHCO_3$ solution, and the mixture was again centrifuged as before. The supernatants were harvested for use in the LDH assay, the mixture for which contained 1.0 unit of LDH, 0.3 mM NADH, and 100 mM potassium phosphate (pH 7.5) in a total volume of 1 ml. Controls for NADH oxidase were run with all reaction mixtures in the absence of added LDH. Any endogenous NADH oxidation was subtracted from the total rate measured. The change in the A_{340} (4-min assay) was used to estimate the remaining concentration of pyruvate.

TABLE 1. PFOR activities with BV and NTZ as electron acceptors[a]

Organism	PFOR sp act		K_i (μM NTZ)
	NTZ	BV	
Trichomonas vaginalis	—[b]	52.5 ± 12	2.2
Entamoeba histolytica	19 ± 5	742.5 ± 67	10
Giardia intestinalis	41.5 ± 4	62.5 ± 14	
Clostridium difficile	18.8 ± 7	105.5 ± 12	
Clostridium perfringens	56.5	225	
Helicobacter pylori	8.5	127	4.5
Campylobacter jejuni	20 ± 2	115 ± 8	10.5

[a] The specific activities obtained with NTZ and BV are in nmoles per min per mg of protein and were obtained with high-speed supernatants. Each activity represents the mean of three determinations obtained from cell extracts prepared from independent experiments. K_i was computed from Dixon plots of $1/V$ versus the concentration of NTZ (in μM).

[b] —, activity was not consistently measured in extracts of *T. vaginalis*.

Mass spectrometry. Samples were prepared for mass spectrometry analysis as pure compounds of NTZ and TIZ in DMSO. Oxidized or enzymatically reduced NTZ or TIZ was prepared as each compound would have been prepared for a normal enzyme assay reaction. Immediately after addition of NTZ or TIZ to the reaction mixture or following enzymatic action, samples were subjected to extraction with 2 volumes of 80% (vol/vol) acetonitrile in borosilicate glass tubes, followed by centrifugation at 8,000 rpm for 10 min at 4°C. For chemical reduction, samples were prepared in 100 mM potassium phosphate (pH 7.5), 0.18 mM CoA, and 5 μM TPP and then reduced with sodium dithionite prior to extraction with acetonitrile. Mass spectra were collected in the negative ion mode.

NMR. ^{1}H NMR data were collected in DMSO-d_6 and in solutions accompanied by trifluoroacetic acid, potassium *tert*-butoxide, or triethylamine.

RESULTS

NTZ is a broad-spectrum antiparasitic drug that also exhibits toxicity against a range of anaerobic bacteria, microaerophiles, and some viruses (5, 8, 20, 21, 22, 27). To test whether PFOR is a general target of NTZ, cellular extracts were prepared from each of the organisms listed in Table 1, and PFOR activities were measured anaerobically by monitoring the reduction of BV at 546 nm or the change in the absorbance at 418 nm for NTZ. The enzyme activities measured were highly reproducible and were optimized for cofactors and substrates. The specific activities measured with BV were generally much higher than those measured with NTZ, and the species variation likely reflects the relative concentration of PFOR in each extract and the influence of other cellular enzymes. PFOR activity, as measured with NTZ, yielded inconsistent results only with cellular extracts from *T. vaginalis*. However, the PFOR of this organism was especially susceptible to inhibition by this drug in BV competition studies ($K_i = 2.2$ μM). Concentration-dependent inhibition of BV reduction by NTZ was demonstrated with extracts from each organism. The K_i for NTZ ranged from 2 to 10 μM and was independent of the BV concentration, consistent with a noncompetitive inhibition mechanism (i.e., NTZ does not compete directly with BV for reducing equivalents).

NTZ is not chemically altered by PFOR. We previously suggested that the observed spectral shift of NTZ from 418 nm to 351 nm during the PFOR reaction might be due to a nitroreduction mechanism (28). To determine whether nitroreduction (of the 5-nitro group of NTZ) had occurred, negative-ion mass spectrometry was used to identify the chemical composition of the 351-nm-absorbing reaction product of the PFOR reaction. The major masses detected included $m/z + 1$ at 306 for NTZ, and peaks at $m/z + 1$ of 264 and 217 represented the loss of the acetyl group (43 amu) and the nitro group, respectively. These values were identical to those obtained with the 418-nm-absorbing compound, indicating that nitroreduction had not occurred. If nitroreduction had occurred, either an oxime (NOH) or an amine (NH_2) would have been produced from the nitro group. The mass spectra showed no ion peaks for either of these two products.

NTZ inhibits *E. coli* growth in MinA medium. In a previous study, we noted that 15 μg/ml of NTZ in a glucose-based MinA medium partly inhibited the growth of *E. coli* strain CC104 expressing the *rdxA* nitroreductase of *H. pylori* (28). Growth inhibition had not been previously noted during MIC testing in LB-based medium, which showed *E. coli* to be resistant to NTZ (MIC > 32 μg/ml). To exclude the possibility that NTZ might be activated by RdxA, *E. coli* strain pGS950 (*rdxA*) and a pBSK-containing control strain were grown in glucose MinA medium containing various concentrations of NTZ and MTZ. We had previously established that *rdxA* expression rendered *E. coli* highly susceptible to killing by MTZ (9, 29). As shown in Fig. 3, MTZ was inhibitory to the growth of *E. coli* pGS950 compared with that for a pBSK-containing control. In contrast, both pGS950- and pBSK-containing strains of *E. coli* were inhibited 35 to 80% in a dose-dependent manner by NTZ. The addition of LB medium to the glucose minimal medium reversed the inhibitory action of NTZ (data not presented). To investigate whether NTZ was inhibitory to pyruvate dehydrogenase, PDH activity was assayed in extracts of strain JVQ2 by using NAD as the electron acceptor. At 20 μM, PDH was inhibited ~22%, sufficient perhaps to account for the partial growth inhibition noted under conditions in which PDH assumes a greater role in central metabolism but not sufficient for therapeutic efficacy, as indicated by the high MIC for *E. coli*. Taken together, these findings essentially rule out nitroreduction as a possible mechanism of action for NTZ and confirm a novel mechanism that is common to the PFOR class and, to a lesser extent, to the PDH class of oxidative decarboxylases.

Kinetic and inhibitor analyses of recombinant *H. pylori* PFOR. Initial velocity data were collected over a range of pyruvate concentrations with NTZ and BV (in excess) as electron acceptors. The apparent K_m for pyruvate with NTZ as the acceptor was 0.29 mM, and that with BV was 0.49 mM (the plots are not presented). These constants were reproducible, did not vary from batch to batch, and are consistent with the constants published elsewhere (15). Initial velocity measurements over a range of NTZ concentrations (with the concentrations of the other substrates held constant) was used to compute an apparent K_m of 45 μM and a V_{max} of ca. 96 nmol per min per mg of protein. The robust PFOR activity noted in extracts prepared from *G. intestinalis* permitted determination of an apparent K_m for NTZ of 44 ± 12 μM (data not presented). Plotting of the reciprocal of the initial velocities of BV reduction at each concentration of NTZ (Dixon plot) produced an apparent K_i of 4.5 ± 1.2 μM for the partially purified PFOR of *H. pylori*, in good agreement with the results depicted in Table 1. These results indicate that NTZ is a noncompetitive inhibitor of PFOR and that the drug is not redox active.

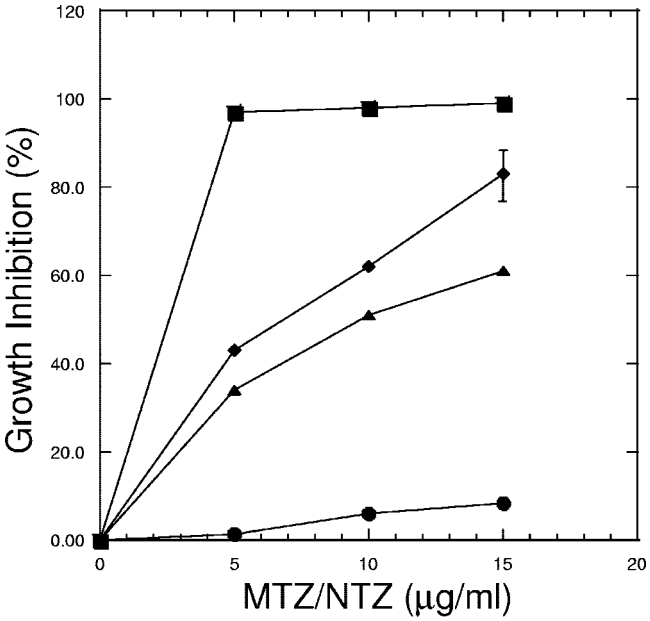

FIG. 3. Effects of MTZ and NTZ on growth of *E. coli* strains expressing the metronidazole reductase gene *rdxA*. Bacterial growth was measured spectrophotometrically at 16 h in glucose MinA medium supplemented with MTZ for *E. coli* pGS950 *rdxA* (■) or pBSK (●) and NTZ for *E. coli* pGS950 *rdxA* (◆) and pBSK (▲). The mean and standard deviation of triplicate measures are plotted as the percentage of growth inhibition versus the inhibitor concentration.

NTZ does not replace TPP. To determine if NTZ, a putative structural analogue of TPP, displaces TPP, PFOR was dialyzed against 10 mM NTZ and 10 mM sodium pyruvate in buffer A with 20% DMSO. As seen in Fig. 4, full enzyme activity (BV reduction) was measured relative to that of the nondialyzed control and relative to that of the DMSO control (Fig. 4, inset). The slight delay in enzymatic activity (~2-min delay) is due to inhibition of BV reduction by residual NTZ. After NTZ was consumed (spectral shift of the 418-nm-absorbing form to the 351-nm form), BV reduction recovered to the levels observed in the absence of inhibitor (Fig. 4). If the TPP had been displaced by NTZ, TPP would have been diluted to extinction by dialysis, thereby inactivating PFOR. These results also established that NTZ is consumed in the PFOR reaction and that the 351-nm-absorbing form is no longer inhibitory.

NTZ inhibits formation of acetyl-CoA. Since NTZ appeared to intercept PFOR prior to reduction of BV, we next examined cofactor requirements. We first established that reduced CoA was required for PFOR activity by showing a concentration-dependent increase in PFOR activity in the standard BV reduction assay (Fig. 5A). However, as also seen in Fig. 5A, reduced CoA was not required for the PFOR reaction with NTZ, suggesting that NTZ intercepts the reaction before binding of reduced CoA. To verify that acetyl-CoA was not a

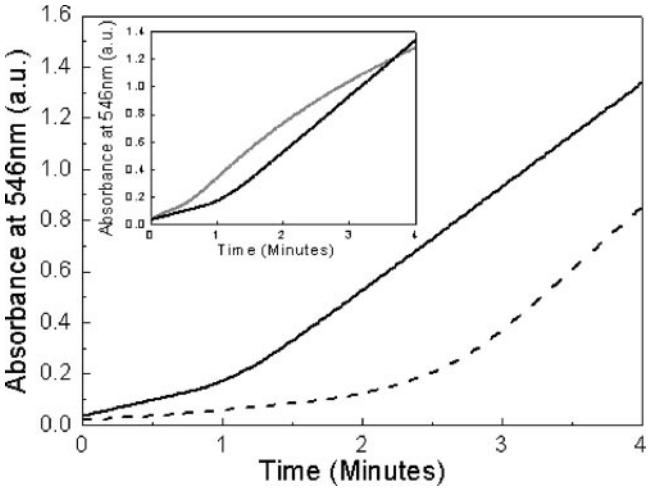

FIG. 4. TPP displacement by NTZ in BV assay. PFOR was dialyzed against 10 mM NTZ in 10 mM sodium pyruvate in buffer A with 20% DMSO (dashed line) and without NTZ as a control (solid line). The effect of DMSO on the specific activity of PFOR was also analyzed (inset) with 20% DMSO (black line) and a control without added DMSO (gray line). The recovery of PFOR activity indicates that excess NTZ did not replace TPP in the PFOR complex. a.u., absorbance units.

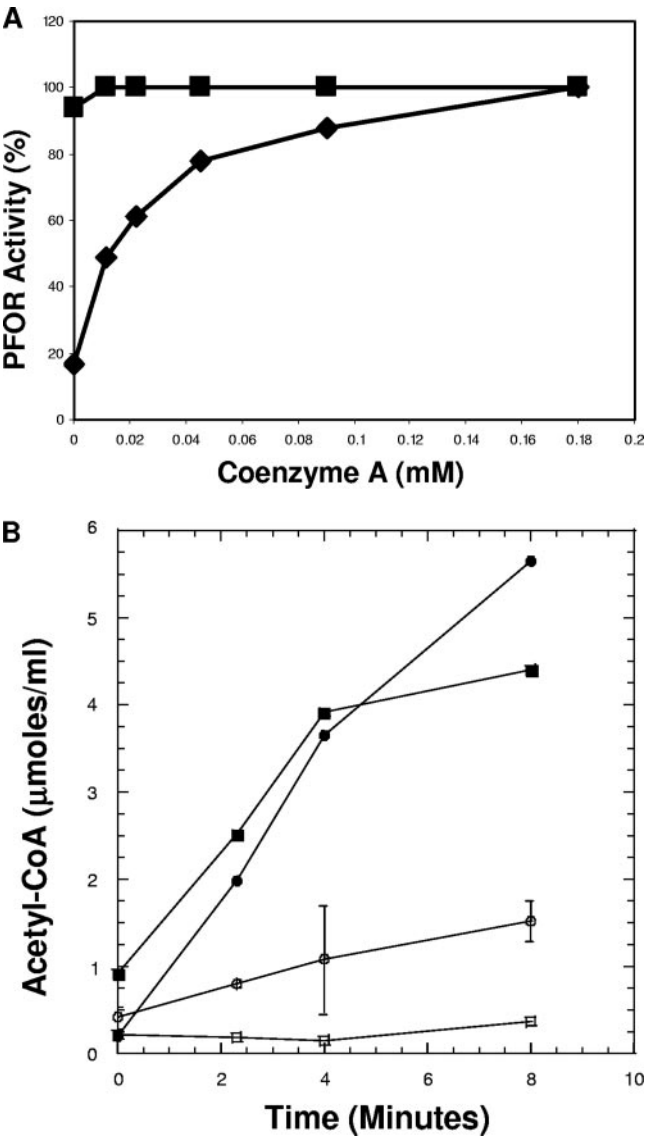

FIG. 5. Reduced CoA cofactor requirement and acetyl-CoA detection. (A) PFOR was assayed with either with BV (♦) or NTZ (■) in the absence and presence of reduced CoA (0 to 0.2 mM). The percent activity is normalized to 100% for uninhibited enzyme activity. (B) Relative accumulation of acetyl-CoA during the PFOR reaction with BV (●), methyl viologen (■), and NTZ (○) as acceptors. The control used was no added pyruvate to the enzymatic reaction (□).

product of the reaction with NTZ, a coupled enzyme assay was used to quantify acetyl-CoA accumulation at intervals during the course of the PFOR reaction. As seen in Fig. 5B, with redox-active dyes (BV and methyl viologen) used as electron acceptors, acetyl-CoA accumulated over the course of the enzyme reaction. In contrast, very little acetyl-CoA was detected in the presence of NTZ, confirming that NTZ likely inhibits PFOR activity at or prior to binding of reduced CoA.

NTZ inhibits pyruvate decarboxylation. The first step of the PFOR reaction is binding of pyruvate to activated enzyme-bound TPP to form the transition intermediate C2-α-lactylthiamine pyrophosphate, which is quickly decarboxylated to produce the hydroxyethyl-TPP radical intermediate. To determine if NTZ acts at or before this step, $^{14}CO_2$ evolution from the decarboxylation of pyruvate was trapped and measured in the presence and absence of NTZ. The results for the DMSO-negative control, TIZ, NTZ, and BV are depicted in Fig. 6. There was no significant increase in CO_2 evolution over that for the controls when the reaction was conducted in the presence of NTZ and TIZ, whereas with BV, significant amounts of $^{14}CO_2$ were generated. Addition of NTZ to the BV assay significantly inhibited the evolution of CO_2, indicating that NTZ inhibits decarboxylation of pyruvate and therefore must inhibit an earlier step.

Pyruvate consumption. Since PFOR activity, as measured spectrophotometrically with either BV or NTZ, is pyruvate dependent, we examined the possibility that NTZ might interfere with the formation of the C2-α-lactyl-TPP reaction intermediate or perhaps chemically change pyruvate to some other product. To test these possibilities, we measured the remaining concentration of pyruvate (substrate) at intervals during the PFOR enzyme reaction by coupling the assay to an NADH-based LDH assay. As seen in Fig. 7, pyruvate was not consumed in the PFOR reaction when NTZ served as the electron acceptor, even though a concurrent change in the absorbance at 418 nm was measured. In contrast, pyruvate was consumed in the PFOR reaction with BV as the electron acceptor (Fig. 7). Since pyruvate was not chemically changed in the reaction with NTZ, NTZ must interfere with the initial binding of pyruvate to the TPP cofactor. Since PFORs are reversible enzymes (formation of pyruvate from CO_2 and acetyl-CoA), NTZ might exert its inhibitory effect by dissociating the putative lactyl-TPP complex prior to decarboxylation.

Chemical basis for spectral shift in NTZ. Clearly, the interaction of NTZ with PFOR causes a molecular change in the drug, as indicated by the spectral shift from 418 nm to 351 nm (even though there is no loss of substrate or accumulation of

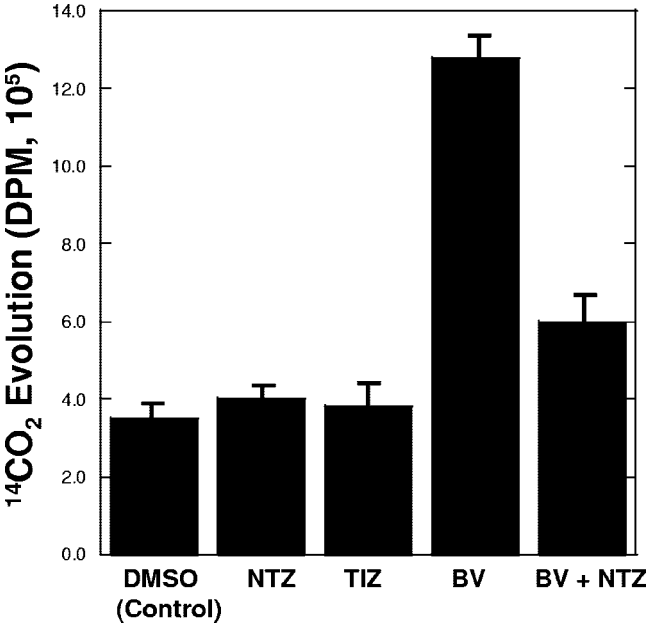

FIG. 6. Evolution of carbon dioxide from the oxidative decarboxylation of pyruvate. Uniformly labeled pyruvate was added to the PFOR reaction with DMSO (negative control), NTZ, TIZ, or BV as the acceptor. The reactions were initiated by addition of [^{14}C]pyruvate, and CO_2 was collected in an NaOH trap and counted by liquid scintillation. The radioactivity of the captured CO_2 is presented in dpm. The reactions were run in triplicate.

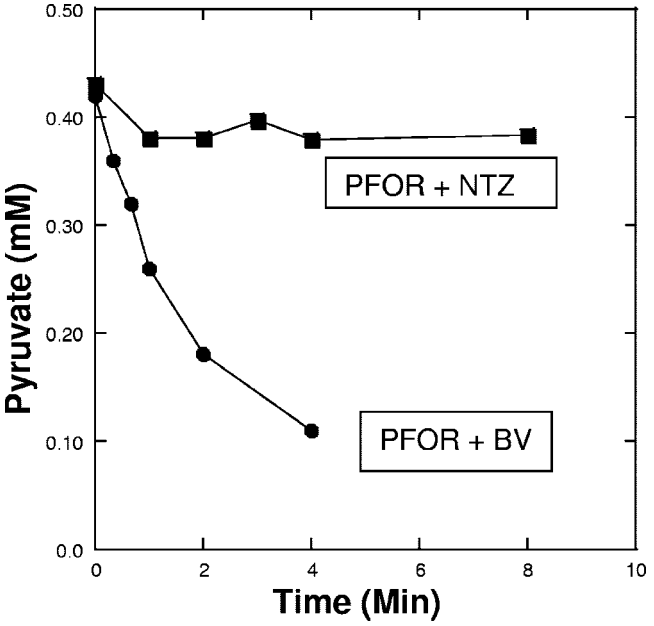

FIG. 7. LDH assay for remaining pyruvate in the PFOR reaction. The standard PFOR reactions were run in the presence of BV and NTZ. The starting concentration of pyruvate was decreased to 0.5 mM. Samples were collected at intervals, proteins were precipitated with perchloric acid, and the neutralized supernatants were assayed for remaining pyruvate by monitoring to completion (4 min) the oxidation of NADH by lactate dehydrogenase. The estimated remaining pyruvate was plotted for each time point of the PFOR reaction. Pyruvate was not consumed in the reaction with NTZ as the electron acceptor.

products); and this change must be relevant to the mechanism of action, since the 351-nm form is inactive. Since the parent compound is yellow in color, we speculated that an electronic rearrangement of the thiazole ring might account for the spectral shift (a loss of color associated with the spectral shift). As seen in Fig. 8A, the optical spectrum of NTZ changes with the pH. At pH 7.4 in 100 mM potassium phosphate buffer, a major absorbance peak at 418 nm is observed. In the same buffer at pH 4.0, the absorbance maximum shifts to 351 nm. The denitro derivative of NTZ displays an absorption maximum at 282 nm that is not influenced by changes in pH (Fig. 8A). The form of NTZ produced in the PFOR reaction showed the same spectral shift from 418 nm to 351 nm in all of the enzyme reactions carried out at pH 7.4 (data not presented). This shift could be reversed by adding the aprotic solvent DMSO to the cuvette, suggesting that the product of the enzyme reaction and the chemical form at pH 4 might be protonated. pH titration experiments indicated that at pH 6.18 (pK_a), both the 418- and 351-nm-absorbing species are equally represented (Fig. 8B), suggesting that NTZ most likely exists as an anion under physiological conditions. ^{1}H NMR analysis of NTZ in DMSO-d_6 under acidic and basic conditions confirmed that the amino group existed as an anion above pH 6 (NTZ^-) and is neutral (HNTZ) under acidic conditions. However, ^{1}H NMR could not distinguish between the two possible tautomers for the protonated HNTZ form (Fig. 9A). Since proton abstraction occurs early in the initial reaction of pyruvate with TPP, we suggest that NTZ most likely intercepts this reaction by protonation. The model depicted in Fig. 9B shows two possible points in the PFOR reaction where proton interception might occur: (i) NTZ reverses the initial binding of pyruvate to the 4′-amino group of amino pyrimidine, or (ii) NTZ attacks the 2-C OH group of C2-α-lactyl-TPP, leading to dissociation of the complex and protonation of NTZ.

DISCUSSION

Here we establish that nitazoxanide is a specific inhibitor of the PFOR class of enzymes found in anaerobic parasites (*G. intestinalis*, *T. vaginalis*, and *E. histolytica*), anaerobic bacteria (*C. difficile* and *C. perfringens*), and members of the epsilon proteobacteria (*H. pylori* and *C. jejuni*). Our findings are consistent with those of previous MIC-based testing, which showed that NTZ and related drugs are active against a broad range of anaerobic bacteria (5, 22), all of which depend on PFOR for pyruvate oxidation. MIC testing also indicates that NTZ is not active against anaerobic gram-positive non-spore-forming rods (*Lactobacillus* spp. and *Propionibacterium* spp.) (22), which lack PFOR, or against strict aerobes and facultative anaerobes which utilize PDH (5). However, the action of NTZ against organisms that utilize PDH might be influenced by nutrition, as the growth of *E. coli* in a glucose minimal medium, but not in LB medium, was substantially inhibited by NTZ. Since therapeutic levels of NTZ inhibited TPP-dependent PDH activity by ~25%, it is likely that other TPP-dependent enzymes, such as pyruvate carboxylase or transketolase, might also be affected, perhaps accounting for the wide therapeutic spectrum noted for this drug (5, 8, 26).

Since NTZ contains a 5-nitro group on the thiazole ring,

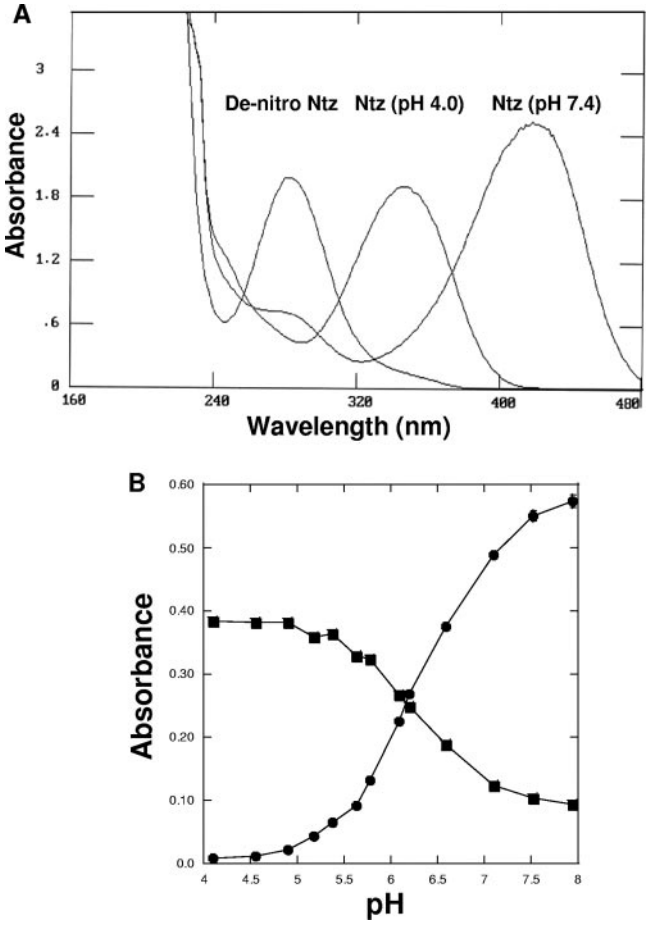

FIG. 8. Absorbance properties of NTZ. (A) The absolute spectra for NTZ at pH 7.4 and 4.0 were recorded with a Cary-14 scanning spectrophotometer from 220 nm to 480 nm. The spectrum for denitro-NTZ was unchanged by pH, and its absorption maximum was at 282 nm. For NTZ, the absorbance maximum at pH 7.4 was 418 nm and that at pH 4.0 was 351 nm. (B) pH titration at 418 nm (●) and 351 nm (■) of a 0.02 mM solution in 10 mM phosphate buffer at the indicated pH values (pK_a = 6.18). The assays were run in triplicate, and the means and standard deviations are indicated.

nitroreduction was considered a likely mechanism of action (28). Generally, nitroreduction involves a $4e^-$ transfer to the nitro group, as demonstrated by the RdxA-catalyzed reduction of MTZ to hydroxylamine (9, 28, 29). Analysis of NTZ products from the PFOR reaction by mass spectrometry indicated that nitroreduction had not occurred, and this conclusion was further supported by the inability of RdxA in *E. coli* to generate toxic or DNA-damaging products of NTZ (29). The nitro group of NTZ is important for biological activity, as substitution with bromine results in a loss of activity against anaerobic bacteria (22) and chemically is due to a loss of resonance in the thiazole ring (the protonated neutral form).

Spectral, NMR, and biochemical studies suggest that NTZ inhibits PFOR activity by a novel mechanism in which the anionic form of the drug interferes with the C2-α-lactyl-TPP intermediate, either before or after formation, causing dissociation of the complex. In the process, the anionic NTZ^- is protonated, resulting in electronic rearrangement of the nitrothiazole ring, detected as a spectral shift from 418 to 351 nm (Fig. 8A). The following lines of experimentation support this conclusion: (i) the activity of NTZ against PFOR was pyruvate dependent, (ii) the substrate (pyruvate) was not consumed or altered chemically in the reaction, (iii) neither CO_2 nor acetyl-CoA was produced as a product of the reaction, (iv) NTZ did not compete for reducing equivalents with redox-active dyes, and (v) the protonated HNTZ form exhibiting an absorbance maximum at 351 nm was no longer biologically active. The HNTZ form could be produced by lowering the pH of the anion in solution from 7.4 to 4.0 (pK_a = 6.18) and regenerated in aprotic solvents. In the absence of enzyme, there was no measurable chemical reaction between NTZ, TPP, and pyruvate. The change in absorbance of NTZ^- in the PFOR reaction was saturable (K_m = 45 μM and 44 μM for the *H. pylori* and *G. intestinalis* PFORs, respectively), and in competition assays, NTZ^- inhibited BV reduction (K_i range, 2 to 10 μM) until NTZ^- was completely converted to HNTZ. The subsequent resumption in BV reduction indicated that NTZ did not replace the TPP cofactor or otherwise permanently affect the PFOR enzyme function.

All PFORs catalyze two successive half-reactions and display ping-pong kinetics in converting pyruvate to CO_2 and acetyl-CoA (2, 3, 23, 24, 25). The catalytic mechanism for the PFOR class of enzymes involves enzyme-bound TPP, which forms a planar "V" configuration in which the 4′-imino group of the aminopyrimidine ring is brought close to the C-2 carbon of the thiazolium ring, leading to the formation of a carbanion following proton abstraction from the C-2 carbon (3, 7, 19, 24, 25). Crystallographic studies by Cavazza et al. with the PFOR of *Desulfovibrio africanus* indicate that pyruvate first binds to the 4′-amino group of the aminopyrimidine ring before activated TPP binds to pyruvate at the C-2 carbon of the thiazole ring, which is then followed by rapid decarboxylation and the release of CO_2 (2) (Fig. 9B). The absence of CO_2 evolution from PFOR in the presence of NTZ suggests that NTZ must intercept this transfer, which causes the displacement of pyruvate, as depicted in the model shown in Fig. 9B. Our studies cannot distinguish whether NTZ inhibits formation of the C2-α-lactylthiamine pyrophosphate intermediate by acquiring a proton from the 4′-amino–pyruvate complex (dissociation restores the imino group) or dissociates pyruvate from the lactyl-TPP complex by attacking the OH group of the lactyl. Further studies with PFOR crystals would be required to determine how NTZ interacts with the transition intermediate. While these studies do not rule out a specific interaction of NTZ with the PFOR enzyme, it is unlikely that iron sulfur centers are involved (the nitro group of NTZ is not redox active), and kinetic data (K_m and K_i) support the formation of an enzyme-substrate complex rather than a nonspecific association with the enzyme.

The selective action of NTZ for PFOR enzymes, as opposed to PDH enzymes, may be a function of the reversibility of the PFOR class of enzymes as well as the tight binding of TPP. For the capnophilic microaerophiles (CO_2-requiring) *H. pylori* and *C. jejuni*, the reverse reaction of PFOR might be favored, as the glycolytic Embden-Myerhof pathway is functional only in the reverse (gluconeogenic) direction due to the absence of pyruvate kinase and the presence of phosphoenolpyruvate syn-

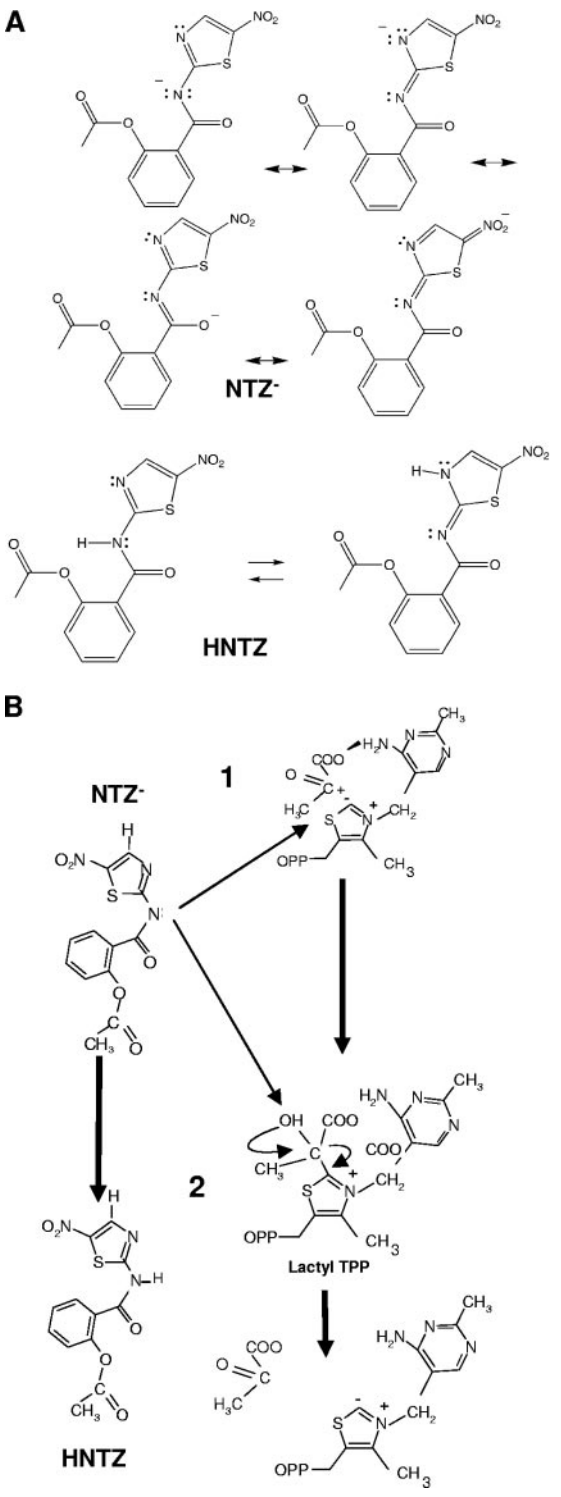

FIG. 9. ^{1}H NMR of NTZ forms and model for NTZ inhibition of PFOR. (A) Two tautomers of protonated HNTZ and four resonance structures of NTZ^- were predicted from ^{1}H NMR. (B) Pyruvate initially interacts with the 4′ amino group of aminopyrimidine (reaction 1), following proton abstraction from the C-2 carbon (the carbanion noted by a negative charge) of the thiazole ring and subsequently forms the C2-α-lactylthiamine pyrophosphate intermediate (reaction 2). Either the anion of NTZ abstracts a proton from reaction 1 (4-amino group), thereby blocking the formation of lactyl-TPP, or, following formation, NTZ becomes protonated, leading to dissociation of the complex and release of pyruvate (reaction 2). Since decarboxylation proceeds rapidly following the formation of lactyl-TPP, NTZ most likely blocks the formation of the C2-α-lactyl-TPP.

thase (*H. pylori*) (12, 30) or, in the case of *C. jejuni*, by an inability to utilize exogenous sugars. Moreover, evidence for carboxylation reactions (isotope exchange reactions with PFOR), first noted for *H. pylori* by Hughes et al. (14), might be explained by the CO_2 fixation capacity of this enzyme. In a separate communication we will report on NADPH-driven pyruvate synthesis by PFOR, flavodoxin, and a novel NADPH oxidase in *H. pylori* and *C. jejuni*. While the information is not presented here, NTZ also blocks the reverse (pyruvate-synthesizing) activity of PFOR, although kinetic details await further study.

In contrast to the rapid development of MTZ resistance by *H. pylori*, attempts to isolate NTZ-resistant mutants of *H. pylori* have not proven successful (19). Similarly, while resistance to most antiparasitic drugs, including MTZ, has been reported clinically (8), no drug resistance has been reported with NTZ usage, although the experience with NTZ is limited so far. If NTZ indeed interacts directly with the activated TPP cofactor, mutations to PFOR would not alter this interaction without altering functional activity, a potentially lethal outcome. Other mechanisms of drug resistance, such as efflux, drug modification, or increased target expression, might still contribute to the development of resistance and will require further monitoring. It might be possible to exploit this putative mechanism by developing new drugs that target the activated TPP cofactors of other TPP-dependent enzymes.

Despite the susceptibility of *H. pylori* strains to NTZ in vitro (MICs, 2 to 8 μg/ml), the drug has little therapeutic efficacy (10). Based on our studies showing that only the anion exhibits biological activity, we suggest that NTZ in the stomach is inactivated (protonated) by gastric acid (pH ~3). As demonstrated in vitro with the pure compound, the inactive compound can be restored to activity by raising the pH, as would happen when stomach contents are alkalinized in the small intestine. The dependence on pK_a for the therapeutic activity of NTZ might affect its clinical efficacy, particularly where variations in local acidity might affect outcomes against target organisms.

In summary, we have established that NTZ is a noncompetitive inhibitor of the PFOR enzymes of anaerobic parasites, anaerobic bacteria, and epsilon proteobacteria. Using the PFOR of *H. pylori* as a model system, we determined that the anionic form of NTZ intercepts pyruvate oxidation prior to decarboxylation, resulting in the dissociation of the TPP-pyruvate complex (releasing pyruvate) and the protonation of NTZ, as depicted in Fig. 9B. Our studies also suggest that NTZ might interfere with other TPP-requiring enzyme reactions, such as the PDH reaction, which might account for the wide spectrum of activity against organisms that do not express PFOR. Conceptually, the targeting of cofactors of enzymatic reactions might prove a novel strategy in the development of new therapeutic agents such as NTZ, for which resistance would be rare or possibly nonexistent.

ACKNOWLEDGMENTS

We thank Ipemida S. Adagu (Sullyman), Marc Ayers, and John-François Rossignol for helpful support and suggestions throughout this study.

This work was supported in part by grants from Romark Laboratories, Inc.; the Canadian Institutes for Health Research; and the Atlantic Innovation Fund and with startup funds from the Faculty of Medicine, University of Virginia (to P.S.H.).

REFERENCES

1. **Adagu, I. S., D. Nolder, D. C. Warhurst, and J. F. Rossignol.** 2002. In vitro activity of nitazoxanide and related compounds against isolates of *Giardia intestinalis*, *Entamoeba histolytica* and *Trichomonas vaginalis*. J. Antimicrob. Ther. **49:**103–111.
2. **Cavazza, C., C. Contreras-Martel, L. Pieulle, E. Chabriere, E. C. Hatchikian, and J. C. Fontecilla-Camps.** 2006. Flexibility of thiamine diphosphate revealed by kinetic crystallographic studies of the reaction of pyruvate-ferredoxin oxidoreductase with pyruvate Structure **14:**217–224.
3. **Chabriere, E., X. Vernede, B. Guigliarelli, M.-H. Charon, E. C. Hatchikian, and J. C. Fontecilla-Camps.** 2001. Crystal structure of the free radical intermediate of pyruvate:ferredoxin oxidoreductase. Science **294:**2559–2563.
4. **Cremades, N., M. Bueno, M. Toja, and J. Sancho.** 2005. Towards a new therapeutic target: *Helicobacter pylori* flavodoxin. Biophys. Chem. **115:**267–276.
5. **Dubreuil, L., X. Houcke, Y. Mouton, and J. F. Rossignol.** 1996. In vitro evaluation of the activities of nitazoxanide and tizoxanide against anaerobes and aerobic organisms. Antimicrob. Agents Chemother. **40:**2266–2270.
6. **Evans, M. C., B. B. Buchanan, and D. I. Arnon.** 1966. A new ferredoxin-dependent carbon reduction cycle in a photosynthetic bacterium. Proc. Natl. Acad. Sci. USA **55:**928–934.
7. **Furdui, C., and S. W. Ragsdale.** 2002. The roles of coenzyme A in the pyruvate:ferredoxin oxidoreductase reaction mechanism: rate enhancement of electron transfer from a radical intermediate to an iron-sulfur cluster. Biochemistry **41:**9921–9937.
8. **Gilles, H. M., and P. S. Hoffman.** 2002. Treatment of intestinal parasitic infections: a review of nitazoxanide. Trends Parasitol. **18:**95–97.
9. **Goodwin, A., D. Kersulyte, G. Sisson, S. J. O. V. van Zanten, D. E. Berg, and P. S. Hoffman.** 1998. Metronidazole resistance in *Helicobacter pylori* is due to null mutations in a gene (*rdxA*) that encodes an oxygen-insensitive NADPH nitroreductase. Mol. Microbiol. **28:**383–394.
10. **Guttner, Y., H. M. Windsor, C. H. Viiala, L. Dusci, and B. J. Marshall.** 2003. Nitazoxanide in treatment of *Helicobacter pylori*: a clinical and in vitro study. Antimicrob. Agents Chemother. **47:**3780–3783.
11. **Hoffman, P. S., and T. G. Goodman.** 1982. Respiratory physiology and energy conservation efficiency of *Campylobacter jejuni*. J. Bacteriol. **150:**319–326.
12. **Hoffman, P. S., A. Goodwin, J. Johnsen, K. Magee, and S. J. O. Veldhuyzen van Zanten.** 1996. Metabolic activities of metronidazole-sensitive and -resistant strains of *Helicobacter pylori*: repression of pyruvate oxidoreductase and expression of isocitrate lyase activity correlate with resistance. J. Bacteriol. **178:**4822–4829.
13. **Horner, D. S., R. P. Hirt, and T. M. Embley.** 1999. A single eubacterial origin of eukaryotic pyruvate:ferredoxin oxidoreductase genes: implications for the evolution of anaerobic eukaryotes. Mol. Biol. Evol. **16:**1280–1291.
14. **Hughes, N. J., P. A. Chalk, C. L. Clayton, and D. J. Kelly.** 1995. Identification of carboxylation enzymes and characterization of a novel four-subunit pyruvate:flavodoxin oxidoreductase from *Helicobacter pylori*. J. Bacteriol. **177:**3953–3959.
15. **Hughes, N. J., C. L. Clayton, P. A. Chalk, and D. J. Kelly.** 1998. *Helicobacter pylori porCDAB* and *oorDABC* genes encode distinct pyruvate:flavodoxin and 2-oxoglutarate:acceptor oxidoreductases which mediate electron transport to NADP. J. Bacteriol. **180:**1119–1128.
16. **Kletzin, A., and M. W. Adams.** 1996. Molecular and phylogenetic characterization of pyruvate and 2-ketoisovalerate ferredoxin oxidoreductases from *Pyrococcus furiosus* and pyruvate ferredoxin oxidoreductase from *Thermotoga maritime*. J. Bacteriol. **178:**248–257.
17. **Mahony, D. E., S. Lim-Morrison, L. Bryden, G. Faulkner, P. S. Hoffman, L. Agocs, G. G. Briand, N. Burford, and H. Maguire.** 1999. Antimicrobial activity of synthetic bismuth compounds against *Clostridium difficile*. Antimicrob. Agents Chemother. **43:**582–588.
18. **Mégraud, F., A. Occhialini, and J. F. Rossignol.** 1998. Nitazoxanide, a potential drug to eradicate *Helicobacter pylori* with no cross resistance to metronidazole. Antimicrob. Agents Chemother. **42:**2836–2840.
19. **Menon, S., and S. W. Ragsdale.** 1996. Unleashing hydrogenase activity in carbon monoxide dehydrogenase/acetyl-CoA synthase and pyruvate:ferredoxin oxidoreductase. Biochemistry **35:**15814–15821.
20. **Musher, D. M., N. Logan, R. J. Hamill, H. L. Dupont, A. Lentnek, A. Gupta, and J. F. Rossingol.** 2006. Nitazoxanide for the treatment of *Clostridium difficile* colitis. Clin. Infect. Dis. **43:**421–427.
21. **Ortiz, J. J., N. Lopez Chegne, G. Gargala, and L. Favennec.** 2002. Comparative clinical studies of nitazoxanide, albendazole and praziquantel in the treatment of ascariasis, trichuriasis and hymenolepiasis in children from Peru. Trans. R. Soc. Trop. Med. Hyg. **96:**193–196.
22. **Pankuch, G. A., and P. C. Appelbaum.** 2006. Activities of tizoxanide and nitazoxanide compared to those of five other thiazolides and three other agents against anaerobic species. Antimicrob. Agents Chemother. **50:**1112–1117.
23. **Patel, M. S., and T. E. Roche.** 1990. Molecular biology and biochemistry of pyruvate dehydrogenase complexes. FASEB J. **4:**3224–3233.
24. **Pohl, M., G. A. Sprenger, and M. Muller.** 2004. A new perspective on thiamine catalysis. Curr. Opin. Biotechnol. **15:**335–342.
25. **Ragsdale, S. W.** 2003. Pyruvate ferredoxin oxidoreductase and its radical intermediate. Chem. Rev. **103:**2333–2346.
26. **Rossignol, J. F., M. Abu-Zekry, A. Hussein, and M. G. Santoro.** 2006. Effect of nitazoxanide for treatment of severe rotavirus diarrhoea: randomised double-blind placebo-controlled trial. Lancet **368:**124–129.
27. **Rossignol, J. F., A. Ayoub, and M. S. Ayers.** 2001. Treatment of diarrhea caused by *Cryptosporidium parvum*: a prospective randomized, double-blind, placebo-controlled study of nitazoxanide. J. Infect. Dis. **184:**103–106.
28. **Sisson, G., A. Goodwin, A. Raudonikiene, N. J. Birks, H. Han, A. Mukhopadhyay, D. E. Berg, and P. S. Hoffman.** 2002. Enzymes associated with the reductive activation and action of nitazoxanide, nitrofurans and metronidazole in *Helicobacter pylori*. Antimicrob. Agents Chemother. **46:**2116–2123.
29. **Sisson, G., J. Y. Jeong, A. Goodwin, L. Bryden, N. Rossler, S. Lim-Morrison, A. Raudonikiene, D. E. Berg, and P. S. Hoffman.** 2000. Metronidazole activation is mutagenic and causes DNA fragmentation in *Helicobacter pylori* and in *Escherichia coli* containing a cloned *H. pylori* RdxA$^+$ (nitroreductase) gene. J. Bacteriol. **182:**5091–5096.
30. **Tomb, J.-F., O. White, A. R. Kerlavage, R. A. Clayton, G. G. Sutton, R. D. Fleischmann, K. A. Ketchum, H. P. Klenk, S. Gill, B. A. Dougherty, K. Nelson, J. Quackenbush, L. Zhou, E. F. Kirkness, S. Peterson, B. Loftus, D. Richardson, R. Dodson, H. G. Khalak, A. Glodek, K. McKenney, L. M. Fitzegerald, N. Lee, M. D. Adams, E. K. Hickey, D. E. Berg, J. D. Gocayne, T. R. Utterback, J. D. Peterson, J. M. Kelley, M. D. Cotton, J. M. Weidman, C. Fujii, C. Bowman, L. Watthey, E. Wallin, W. S. Hayes, M. Borodovsky, P. D. Karp, H. O. Smith, C. M. Fraser, and J. C. Venter.** 1997. The complete genome sequence of the gastric pathogen *Helicobacter pylori*. Nature **388:**539–547.
31. **Townson, S. M., J. A. Upcroft, and P. Upcroft.** 1996. Characterization and purification of pyruvate:ferredoxin oxidoreductase from *Giardia duodenalis*. Mol. Biochem. Parasitol. **79:**183–193.
32. **Uyeda, K., and J. C. Rabinowitz.** 1971. Pyruvate-ferredoxin oxidoreductase. 3. Purification and properties of the enzyme. J. Biol. Chem. **246:**3111–3119.
33. **Whiteway, J., P. Koziarz, J. Veall, N. Sandhu, P. Kumar, B. Hoecher, and I. B. Lambert.** 1998. Oxygen-insensitive nitroreductases: analysis of the roles of *nsfA* and *nfsB* in development of resistance to 5-nitrofuran derivatives in *Escherichia coli*. J. Bacteriol. **180:**5529–5539.
34. **Yamamoto, Y., A. Hakki, H. Friedman, S. Okubo, T. Shimamura, P. S. Hoffman, and J. F. Rossignol.** 1999. Nitazoxanide, a nitrothiazolide antiparasitic drug, is an anti-*Helicobacter pylori* agent with anti-vaculating toxin activity. Chemotherapy **45:**303–312.
35. **Zulu, I., P. Kelly, L. Njobvu, S. Sianongo, K. Kaonga, V. McDonald, M. Farthing, and R. Pollok.** 2005. Nitazoxanide for persistent diarrhea in Zambian acquired immune deficiency syndrome patients: a randomized-controlled trial. Aliment. Pharmacol. Ther. **21:**757–763.